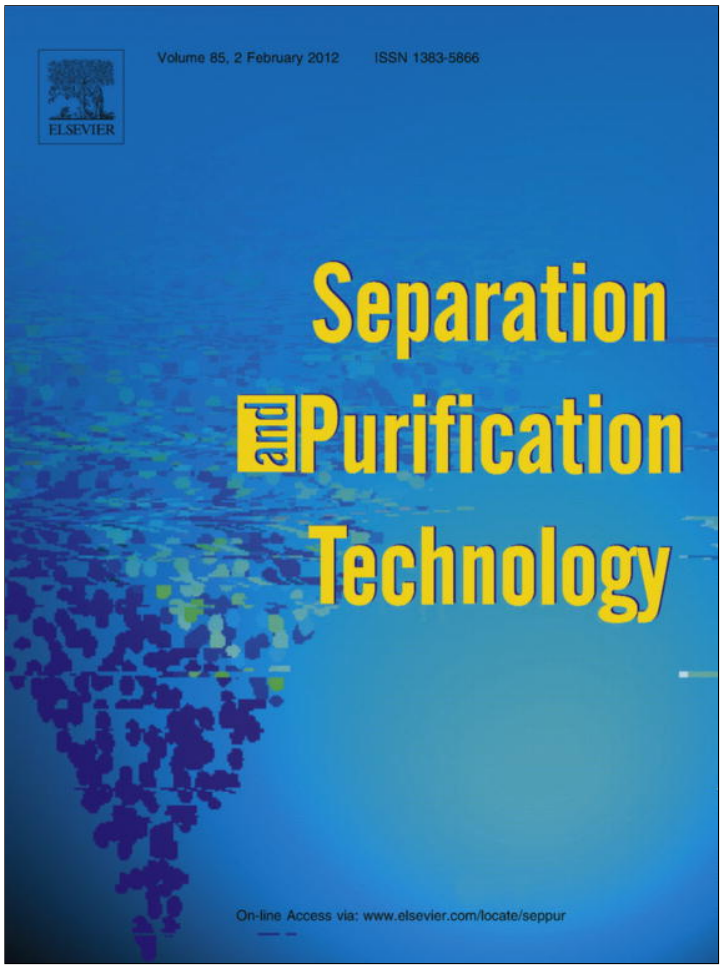

(This is a sample cover image for this issue. The actual cover is not yet available at this time.)

Separation and Purification Technology 108 (2013) 189–195

Contents lists available at SciVerse ScienceDirect

Separation and Purification Technology

journal homepage: www.elsevier.com/locate/seppur

Removal of Cu(II) ions from aqueous solution using sulfonated magnetic graphene oxide composite

Xin-jiang Hu, Yun-guo Liu *, Hui Wang, An-wei Chen, Guang-ming Zeng, Si-mian Liu, Yi-ming Guo, Xi Hu, Ting-ting Li, Ya-qin Wang, Lu Zhou, Shao-heng Liu

College of Environmental Science and Engineering, Hunan University, Changsha 410082, PR China
Key Laboratory of Environmental Biology and Pollution Control (Hunan University), Ministry of Education, Changsha 410082, PR China

ARTICLE INFO

Article history:
Received 7 September 2012
Received in revised form 10 November 2012
Accepted 11 February 2013
Available online 18 February 2013

Keywords:
Graphene oxide
Sulfonated
Magnetic
Cu(II) removal
Adsorption

ABSTRACT

Graphene oxide has received world-wide attention due to its exceptional physicochemical properties. Herein, a sulfonated magnetic graphene oxide composite (SMGO) was synthesized from graphene oxide and was used as adsorbent for removing Cu(II) ions from aqueous solution. The composite was characterized by TEM, EDS, particles size, BET, TG-DTA, FT-IR, and Raman. It can be separated and recovered easily using magnetic separation technology. The effects of operating parameters such as pH, Cu(II) concentration and temperature on the Cu(II) adsorption were investigated by using a response surface methodology (RSM). Optimum Cu(II) uptake of 62.73 mg g^{-1} was achieved at pH 4.68, Cu(II) concentrations 73.71 mg L^{-1}, and temperature 50 °C. The adsorption process can be well described by the pseudo-second order kinetic model. The experimental data of isotherm followed the Langmuir isotherm model. Moreover, the thermodynamic parameters calculated from the temperature-dependent isotherms indicated that the adsorption reaction was an endothermic and spontaneous process. All results indicate that the SMGO is a promising adsorbent for the efficient removal of copper ions from wastewater.

1. Introduction

Graphene oxide (GO), also called graphite oxide sheet, is a two dimensional nanomaterial prepared from chemical oxidation of natural graphite [1,2]. In contrast to pristine graphite, the graphene oxide sheets are heavily oxygenated, bearing hydroxyl and epoxide functional groups on their basal planes, in addition to carbonyl and carboxyl groups located at the sheet edges [3–5]. These groups and the large surface area of GO hold great promise for removal and recovery of metals from aqueous solutions [6]. Some researchers have applied GO and GO based composite materials to the removal of various metal ions, such as chromium(VI) [7], copper(II) [8], lead(II) [9], cadmium(II) and cobalt(II) [6]. However, owing to its hydrophilic nature, GO can be dispersed in aqueous media, it is difficult to be separated from the solution using traditional separation methods after the adsorption process, which may increase the cost of industrial application and/or cause the treated water to be re-polluted [3,10]. The problem can be solved using magnetic technology [11]. The magnetic properties of some magnetic materials such as Fe_3O_4 and γ-Fe_2O_3 can be imparted to adsorbents facilitating their trapping from the medium with the help of an external magnetic field [12]. This technology combines the advantages of adsorption with the merit of easy separation due to the incorporation of magnetic species [10].

The ability of an adsorbent to capture metals is controlled in part by the number and the kind of available functional groups used for binding metals [13]. The groups on the GO backbone are very limited, which may cause trouble in its application for removal of metal ions. Therefore, it is highly needed to find a method to introduce some stable and specific functional moieties to GO [14]. In order to increase the adsorption ability of GO, and to improve the adsorption selectivity of metal ions, a great number of GO derivates have been obtained by grafting new functional groups such as ethylenediamine [7] and EDTA [9] through a GO backbone. Sulfanilic acid is widely used in the manufacture of dyes, pesticides and sulpha drugs. It contains a sulfo group ($-SO_3H$) and an amino group ($-NH_2$). The amino group can react with cold nitrous acid to produce diazotized sulfanilic acid which can be used to synthesize the sulfonated magnetic graphene oxide composite. The sulfo group on the benzene ring is known to form stable complexes with various metal cations. Therefore the sulfonated magnetic graphene oxide composite may be favorable for the metal cations removal. Copper exists mainly as divalent cation in aqueous solutions. Water containing copper beyond the prescribed limit of 1.3 mg L^{-1} causes liver damage and lung cancer in human

* Corresponding author at: College of Environmental Science and Engineering, Hunan University, Changsha 410082, PR China. Tel.: +86 731 88649208; fax: +86 731 88822829.
E-mail address: hnuese@126.com (Y.-g. Liu).

1383-5866/$ - see front matter © 2013 Elsevier B.V. All rights reserved.
http://dx.doi.org/10.1016/j.seppur.2013.02.011

beings [15]. Therefore, it is necessary to treat copper contaminated wastewater prior to its discharge to the environment. In the present study, sulfonated magnetic graphene oxide composite was synthesized in an attempt to remove Cu(II) ions from aqueous solution.

The objectives of this study were to (1) prepare and characterize sulfonated magnetic graphene oxide composite (SMGO) and apply it as adsorbent to remove Cu(II) ions from aqueous solution in a batch system; (2) model and optimize the adsorption process with RSM technique; (3) investigate the effects of the process parameters on Cu(II) adsorption; (4) discuss the adsorption mechanism with kinetic, isotherm and thermodynamic models.

2. Materials and methods

2.1. Materials

Graphite powder was supplied by Tianjin Hengxin Chemical Preparation Co., Ltd. Sulfanilic acid was provided by Tianjin Guangfu Fine Chemical Research Institute, Tianjin, China. All chemicals used in the experiments were analytical grade.

GO was synthesized by oxidizing natural flake graphite powder using a modified Hummers method [2,8,9]. Briefly, graphite powders were first preoxidized by concentrated H_2SO_4, $K_2S_2O_8$, and P_2O_5. Next, the concentrated H_2SO_4, $KMnO_4$ and $NaNO_3$ were used to oxidize the preoxidized graphite, and 30% H_2O_2 was added to eliminate the excess MnO_4^-, and the products were rinsed with HCl (10%) and Milli-Q water and then sonicated for 2 h. The magnetic graphene oxide (MGO) was prepared by coprecipitation method. Fe^{3+} and Fe^{2+} (molar ratio 2:1) were mixed in the GO solution with addition of ammonia solution to form Fe_3O_4-GO composite. The sulfonated magnetic graphene oxide composite (SMGO) was obtained by reacting aryl diazonium salt of sulfanilic acid with MGO in ice bath for 4 h. The reaction mechanism of MGO with aryl diazonium salt of sulfanilic acid involves the homolytic fission of dinitrogen from the diazonium salt leading to the generation of aryl radical which binds to the MGO surface via stable C—C covalent bond [16]. The resulted paste was filtered and washed repeatedly until pH was about 7.0 and finally stored at 4 °C. The concentration of SMGO, which was used for adsorption in our experiment, was 4.50 ± 0.16 mg mL^{-1}. Detailed processes are illustrated in the Supplementary Data.

2.2. Characterization

The TEM image was performed on a JEOL1230 microscope. The EDS spectrum was collected with an energy-dispersive X-ray spectrometer (EDAX Genesis 2000, USA). The size of the adsorbent was obtained by Zeta Sizer and Nano series equipped with a microprocessor unit (ZEN3690, Malvern, UK). The BET specific surface area was determined using nitrogen adsorption–desorption measurements (Autosorb-1, Quantachrome Instruments, USA). TG and DTA curves were recorded using thermoanalytical equipment (SDT Q600, USA) in nitrogen atmosphere from room temperature to 800 °C (sample mass 19.350 mg, flux rate 100 mL min^{-1}, heating rate 10 °C min^{-1}). FT-IR spectrum of SMGO was collected by using a Perkin–Elmer Spectrum One spectrometer in KBr pellet at room temperature. The Raman spectra were carried out using a Raman spectrometer (Labram-010, JY, FAR).

2.3. Batch adsorption procedures

The stock solution (1 g L^{-1}) of Cu(II) was prepared by dissolving pure copper powder (1.000 g of pure copper powder was dissolved in 20 mL HNO_3 solution (20%) in a 1000 mL flask and Milli-Q water was added up to the mark). The solutions of different concentrations used in various experiments were obtained by diluting stock solution.

For all the adsorption experiments, 2 mL (0.45 ± 0.16 mg mL^{-1}) of SMGO were introduced into 50 mL of the Cu(II) solution in conical flasks, and the experiments continued on a rotary shaker (180 r min^{-1}) at 30 °C for 6 h. Then, the mixture was separated by using a permanent magnet. The concentration of Cu(II) ions was determined by flame atomic absorption spectrometry (Perkin-Elmer AA700, USA). The effects of pH (3.0–6.0), Cu(II) concentration (20–80 mg L^{-1}), and temperature (10–50 °C) on the q_e (according to Eq. (1)) were investigated by response surface methodology.

$$q_e = \frac{(C_0 - C_e)V}{W} \quad (1)$$

where q_e is the equilibrium adsorption capacity (mg g^{-1}), C_0 and C_e are the initial and equilibrium liquid phase solute concentration (mg L^{-1}), respectively. V is the liquid phase volume (L) and W is the amount of adsorbent (g).

2.4. Box–Behnken experimental design and method of analysis

The relationship between factors and responses was established by empirical mathematical models based on the response surface methodology (RSM). Box–Behnken design (BBD) is a class of rotatable or nearly rotatable second-order designs based on three-level, incomplete factorial design, and it is the most frequently used under response surface method (RSM) design [17]. Based on the results from preliminary experiments, a three-factor, three-level Box–Behnken experimental was employed to model and optimize the adsorption process. The three factors (pH, Cu(II) concentration, and temperature) are represented by X_1, X_2, and X_3, respectively. Adsorption capacity (q_e, Y) was taken as the response. Factors and their levels were shown in Supplementary Data Table S1 and total of 18 experiments were performed (Table 1) including six center points for replication. Experimental data obtained from the BBD model experiments can be stated in the form of the following equation:

$$Y = \beta_0 + \sum_{i=1}^{3}\beta_i X_i + \sum_{i=1}^{3}\beta_{ii} X_i^2 + \sum_{i=1}^{2}\sum_{j=2}^{3}\beta_{ij} X_i X_j + e \quad (2)$$

Table 1
Experimental design based on Box-Behnken design (BBD) used in this study.

Expt. no.	Coded variables[a]			Responses[b]		
	X_1	X_2	X_3	Y_{Obs}	Y_{Pre}	$Y_{Obs}-Y_{Pre}$
1	−1(3.0)	−1(20)	0(30)	25.37 ± 0.89	24.49	0.88
2	1(5.0)	−1(20)	0(30)	37.96 ± 0.70	38.73	−0.76
3	0(3.0)	1(80)	0(30)	41.20 ± 0.42	40.44	0.76
4	1(5.0)	1(80)	0(30)	53.61 ± 0.56	54.49	−0.88
5	−1(3.0)	0(50)	−1(10)	32.04 ± 0.98	32.95	−0.91
6	1(5.0)	0(50)	−1(10)	46.30 ± 1.37	45.57	0.73
7	−1(3.0)	0(50)	1(50)	42.31 ± 3.45	43.04	−0.73
8	1(5.0)	0(50)	1(50)	59.63 ± 0.70	58.72	0.91
9	0(4.0)	−1(20)	−1(10)	32.41 ± 0.89	32.37	0.035
10	0(4.0)	1(80)	−1(10)	46.85 ± 0.98	46.70	0.15
11	0(4.0)	−1(20)	1(50)	42.31 ± 0.70	42.47	−0.15
12	0(4.0)	1(80)	1(50)	59.81 ± 1.12	59.85	−0.035
13	0(4.0)	0(50)	0(30)	52.41 ± 1.25	50.77	1.64
14	0(4.0)	0(50)	0(30)	50.37 ± 0.58	50.77	−0.40
15	0(4.0)	0(50)	0(30)	51.76 ± 1.25	50.77	0.99
16	0(4.0)	0(50)	0(30)	51.02 ± 0.42	50.77	0.25
17	0(4.0)	0(50)	0(30)	49.63 ± 1.05	50.77	−1.14
18	0(4.0)	0(50)	0(30)	49.44 ± 1.27	50.77	−1.33

[a] X_1 = pH, X_2 = Cu(II) concentration (mg L^{-1}), X_3 = Temperature (°C).
[b] Y_{Obs} = Observed values of the adsorption capacity (mg g^{-1}), Y_{Pre} = Predicted values (mg g^{-1}), $Y_{Obs}-Y_{Pre}$ = Residual of observed and predicted values (mg g^{-1}).

where Y represents the value of the response (q_e), and β_0 is the constant coefficient, β_i, β_{ii}, and β_{ij} are the linear, quadratic and interaction coefficients, respectively. X_i and X_j are the levels of the independent variables [18]. The experimental data were analyzed by the Response Surface method with Design-Expert 8.0.6 (Stat-Ease Inc., Minneapolis, MN, USA).

2.5. Modeling of adsorption kinetics, isotherms, and thermodynamics

To evaluate the mechanism of Cu(II) adsorption and the potential rate-controlling steps, such as mass transport and chemical reaction processes, the pseudo-second order and intraparticle diffusion models have been exploited to analyze the experimental data. The pseudo-second order equation based on adsorption equilibrium capacity assumes that the rate of occupation of adsorption sites is proportional to the square of the number of unoccupied sites [19]. The pseudo-second order model can be expressed in the non-linear form:

$$q_t = \frac{q_e^2 K_2 t}{1 + q_e K_2 t} \tag{3}$$

where k_2 is the pseudo-second order adsorption rate constant (g mg^{-1} min^{-1}), and q_e is the adsorption capacity calculated by the pseudo-second order model (mg g^{-1}). The intraparticle diffusion model can be defined as:

$$q_t = k_p t^{1/2} + C \tag{4}$$

where k_p is the intraparticle diffusion rate constant (mg g^{-1} min$^{-0.5}$) and C of adsorption constant is the intercept.

In order to investigate the efficacy of adsorption, Langmuir and Freundlich models have been used to fit experimental data. The Langmuir model assumes that a monomolecular layer is formed when adsorption takes place without any interaction between the adsorbed molecules [20]. The Langmuir model can be represented as:

$$q_e = \frac{q_{max} K_L C_e}{1 + K_L C_e} \tag{5}$$

where K_L is a constant related to the affinity of the binding sites (L mg^{-1}), C_e is the equilibrium concentration (mg L^{-1}), q_e is the amount of metal ion sorbed (mg g^{-1}), q_{max} is q_e for a complete monolayer (mg g^{-1}). The Freundlich model assumes a heterogeneous adsorption surface and active sites with different energy [12]. The Freundlich model is given as:

$$q_e = K_F C_e^n \tag{6}$$

where, K_F and n are the Freundlich constants which are related to adsorption capacity and intensity, respectively.

The thermodynamic parameters (ΔG°, ΔH°, and ΔS°) provide in-depth information about internal energy changes that are associated with adsorption [21]. The standard free-energy change (ΔG°) can be calculated from the following equation:

$$\Delta G^\circ = -RT \ln K^\circ \tag{7}$$

where R is the universal gas constant (8.314 J mol^{-1} K^{-1}), T is the absolute temperature (K), K° is the adsorption equilibrium constant (it can be calculated by plotting ln K_d ($K_d = q_e/C_e$) versus C_e and extrapolating C_e to zero [6]. The standard enthalpy change (ΔH°) and the standard entropy change (ΔS°) are calculated from the following equation:

$$\ln K^\circ = -\frac{\Delta H^\circ}{RT} + \frac{\Delta S^\circ}{R} \tag{8}$$

The slope and intercept of the plot of ln K° versus 1/T are $-\Delta H^\circ/R$ and $\Delta S^\circ/R$, respectively [21,22].

3. Results and discussion

3.1. Characterization of the composite

The TEM photograph (Fig. 1a) shows that large quantities of Fe_3O_4 particles are deposited on the GO surface. Besides, some wrinkles are observed on the surface of the composite. The inset of Fig. 1a shows that the obtained SMGO can be easily collected by a permanent magnet. The EDS spectrum (Fig. 1b) of SMGO shows that the major constituents of the composite are C, O, S, and Fe. The C mainly comes from the GO sheets, while O from both Fe_3O_4 and the oxygen-containing functional groups of GO, and the S mainly comes from the sulfo group of sulfanilic acid. The size distribution of SMGO is presented in Fig. 1c. The mean diameter of the SMGO was 637 nm. The BET surface area of the SMGO was measured to be 92.79 m^2 g^{-1}. The TG-DTA curves of SMGO (Fig. 1d) shows significant weight loss (14.69%) between 22 and 127 °C, which is attributed to the dehydration process. SMGO was found to have 29.18 wt% weight loss when the temperature range from 127 to 800 °C, which was due to the loss of the functional groups such as carboxyl, epoxide, hydroxyl and sulfo groups on the sheets [23]. FT-IR spectrum of SMGO is shown in Fig. 1e. The peak at ca. 1730 cm^{-1} corresponding to C=O of carboxyl group on the GO shifts to 1638 cm^{-1} may be due to the formation of $-COO^-$ after coating with Fe_3O_4 [24]. The absorptions due to the O–H bending vibration, epoxide groups and skeletal ring vibrations are observed around 1617 cm^{-1} [25]. The absorption at 1400 cm^{-1} may be attributed to tertiary C–OH groups [26]. The peaks at 1133, 1008, and 839 cm^{-1} (two υ_{S-O} and one $\upsilon_{S-phenyl}$) confirmed the presence of $-SO_3-$ group [2]. The peak at 623 cm^{-1} is a characteristic peak corresponding to the stretching vibration of Fe–O [12]. Fig. 1f shows Raman spectra of GO and SMGO. For both of samples, the Raman spectra displays two prominent peaks at ca. 1338 and 1590 cm^{-1}, which are assigned to the D band and G band, respectively. It is well known that the G band is usually assigned to the E_{2g} mode observed for sp^2 carbon domains, while the D band is related to the vibrations of sp^3 carbon atoms of defects and disorder that can break the symmetry and selection rule [10,27]. Usually, the intensity ratio of D (I_D) and G bands (I_G) could be used to measure the extent of disorder. The I_D/I_G of SMGO is slightly higher than that of the GO, because of the introduction of abundant sulfo groups to the sp^2 carbon network [28].

3.2. RSM approach for optimization of Cu(II) adsorption

Table 1 shows the results of BBD experiments for studying the effect of three independent variables along with the predicted mean and observed responses. According to the designed experimental data, the second-degree polynomial model for the adsorption capacity was regressed and obtained as:

$$\begin{aligned} Y_{Pre}(\text{adsorption capacity}) = {} & 50.77 + 7.07X_1 + 7.93X_2 \\ & + 5.81X_3 - 0.046X_1X_2 \\ & + 0.76X_1X_3 + 0.76X_2X_3 \\ & - 5.76X_1^2 - 5.48X_2^2 + 0.054X_3^2 \end{aligned} \tag{9}$$

where X_1, X_2, and X_3 represent the values (in coded units) of pH, Cu(II) concentration and temperature, respectively. ANOVA (Table 2) showed that this regression is statistically significant at F-value of 106.20 and values of prob > F (<0.0001). The well fit of the model was evaluated by the coefficient of determination. In this case, the coefficient (R^2 = 0.9917) and adjusted coefficient (Adj R^2 = 0.9824) are very high, indicating high correlation between the observed and the predicted value [29]. At the same time, a relatively low value of the coefficient of variation (CV = 2.72%) indicates the

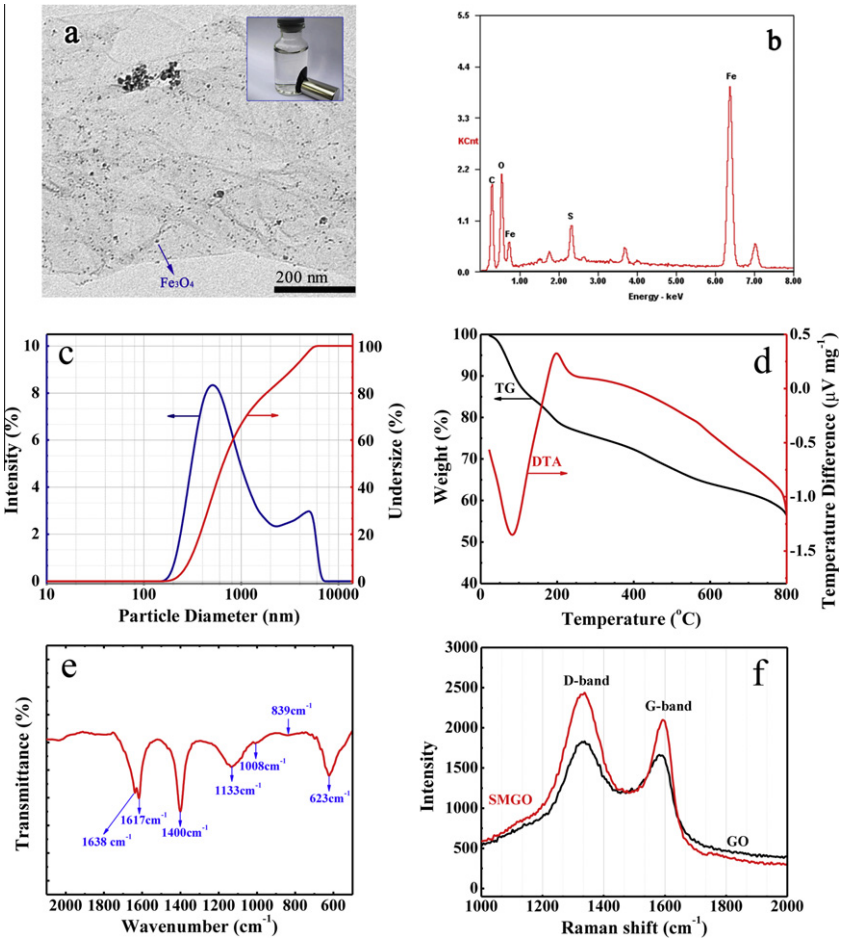

Fig. 1. Characterization of SMGO: (a) TEM photograph; (b) EDS spectrum; (c) Particles size distribution; (d) TG-DTA curves; (e) FT-IR spectrum and (f) Raman spectra of GO and SMGO.

Table 2
Analysis of variance (ANOVA) for response surface quadratic model for Cu(II) removal by the SMGO.

Source	Sum of squares	*df*	Mean square	*F*-Value	*p*-Value[a]
Model	1485.83	9	165.09	106.20	<0.0001
X_1 (pH)	400.08	1	400.08	257.36	<0.0001
X_2 (Cu(II) concentration)	502.86	1	502.86	323.47	<0.0001
X_3 (Temperature)	270.07	1	270.07	173.73	<0.0001
X_1X_2	8.573×10^{-3}	1	8.573×10^{-3}	5.515×10^{-3}	0.9426
X_1X_3	2.33	1	2.33	1.50	0.2553
X_2X_3	2.33	1	2.33	1.50	0.2553
X_1^2	144.58	1	144.58	93.01	<0.0001
X_2^2	130.96	1	130.96	84.25	<0.0001
X_3^2	0.013	1	0.013	8.189×10^{-3}	0.9301
Residual	12.44	8	1.55		
Lack of fit	5.50	3	1.83	1.32	0.3657
Pure error	6.94	5	1.39		

R^2 = 0.9917; Adj R^2 = 0.9824, Pred R^2 = 0.9346, Coefficient of variance = 2.72%.
[a] $p < 0.01$, highly significant; $0.01 < p < 0.05$ significant; $p > 0.05$, not significant.

precision and reliability of the experiments [30]. Besides, the *F*-value for lack-of-fit is insignificant ($p = 0.3657 > 0.05$) thereby confirming the validity of the model. To summary, the quadratic model is statistically significant for the prediction of the adsorption capacity. Fig. 2 also indicates that the values of the responses predicted from the quadratic model agree well with the observed values in the range of the operating variables investigated.

The best way of expressing the effects of the independent variable on the response is to generate surface response plots, which were done by varying two variables within the experimental at its "0" level [17]. Fig. 3a shows the interactive effect of pH and Cu(II) concentration on the adsorption process. According to Fig. 3a, the adsorption capacity of SMGO increased when pH increased from 3 to 5. It can be explained that because the solution pH affects the solution chemistry of metals and the activity of the functional groups of the SMGO. In low pH environments, some functional groups, such as hydroxyl, sulfo, and carbonyl, would be in protonated cationic forms which repel the positively charged

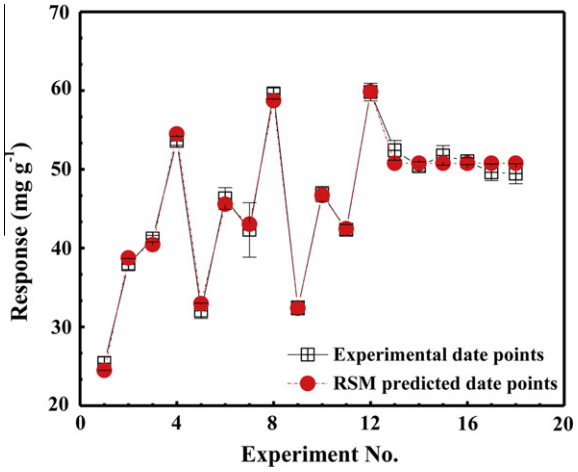

Fig. 2. Comparison between the experimental and predicted values for Cu(II) removal using RSM models.

copper ions. Besides, there is a high concentration of H^+ and H^3O^+, which compete with Cu^{2+} for the binding sites on the surface of the adsorbent, resulting in a decreased adsorption of Cu(II) [11]. With an increase of the pH value, the number of H^+ and H^3O^+ and the potential decreased, resulting in an increase of the adsorption capacity for copper ions [31]. At initial Cu(II) concentrations in the range of 20–60 mg L^{-1}, the adsorption capacity increased with the increase of initial Cu(II) concentration. It can be explained that higher concentration of metal ions enhanced the mass transfer driving force and the number of collisions between Cu(II) ions and the adsorbent, which increased the adsorption process. Concentrations beyond 60 mg L^{-1} made little contributions to the adsorption, which may be due to the saturation of the adsorption sites. Fig. 3b shows the interaction effect of initial solution pH and temperature on the Cu(II) uptake in the form of a 3D plot. As seen in Fig. 3b, over the temperature tested (10–50 °C), higher temperature enhanced the surface activity of the adsorbent and kinetic energy of the solution, resulting in an increased adsorption of Cu(II). This phenomenon indicated that this process is temperature dependent. From Fig. 3c, we can see that the effects of the initial Cu(II) concentration and temperature were similar to Fig. 3a and b. From the regression Eq. (9) and Fig. 3, the optimum conditions for maximum removal (62.73 mg g^{-1}) were found to be as follows: pH 4.68, initial Cu(II) concentrations 73.71 mg L^{-1}, and temperature 50 °C.

3.3. Adsorption kinetics

The adsorption of Cu(II) from aqueous solution to the SMGO as a function of contact time is shown in Fig. 4a. As presented in the figure, the adsorption equilibrium was reached within 180 min. Further increase of contact time cannot lead to stronger adsorption capacity. The fast sorption velocity indicates that strong chemisorption or strong surface complexation contributes to the sorption of Cu(II) on the SMGO [32]. Data on the adsorption rates of Cu(II) ions by various graphene oxide-based composite have shown a wide range of adsorption times. For example, the copper adsorption equilibrium time on graphene oxide aerogels was 15 min [33]. But it was 7 h for graphene oxide/Fe_3O_4 composites [34].

The non-linearized form of the pseudo-second order model for the adsorption is given in Fig. 4a. The value of k_2, q_e was calculated as 1.63×10^{-3} (g mg^{-1} min^{-1}) and 55.205 (mg g^{-1}), respectively. The calculated q_e values agreed very well with the experimental data. Besides, the correlation coefficient was 0.989. Therefore, the

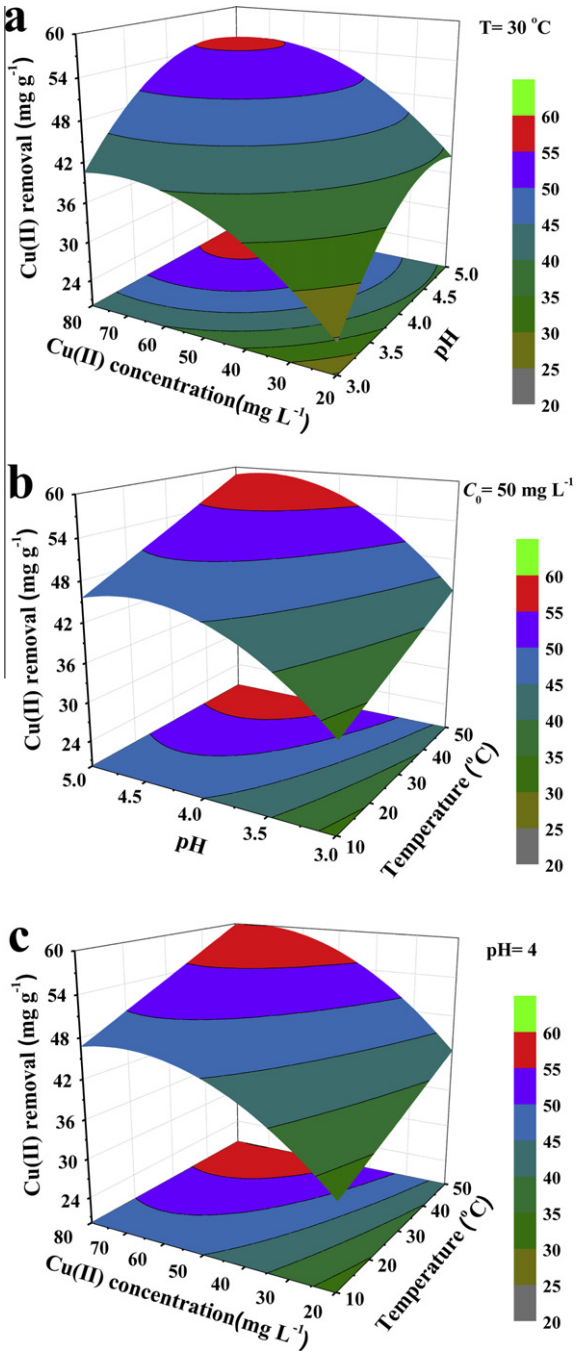

Fig. 3. 3D surface mapping plot for multiple effect of (a) pH and Cu(II) concentration (m/V = 0.18 g L^{-1}, t = 6 h, T = 30 °C), (b) pH and temperature (m/V = 0.18 g L^{-1}, t = 6 h, C_0 = 50 mg L^{-1}), (c) Cu(II) concentration and temperature (m/V = 0.18 g L^{-1}, t = 6 h, pH = 4.0).

kinetic data for the adsorption process obeyed the pseudo-second order model, suggesting a chemisorption process [35]. A similar observation was previously reported by Prasanna Kumar et al. [36] for copper(II) sorption onto *Tectona grandis* L. f. leaves powder. It is more likely to predict that the adsorption behavior may involve valency forces through sharing or exchange of electrons between metal cations and the functional groups of SMGO [36].

The intraparticle diffusion model was used to identify the mass transfer steps in the Cu(II) ions adsorption onto SMGO. The plot of q_t versus $t^{0.5}$ is observed in Fig. 4b. As reported, if the regression of q_t against $t^{0.5}$ is linear and the regression line passes through the origin, then it can be concluded that the intraparticle diffusion is

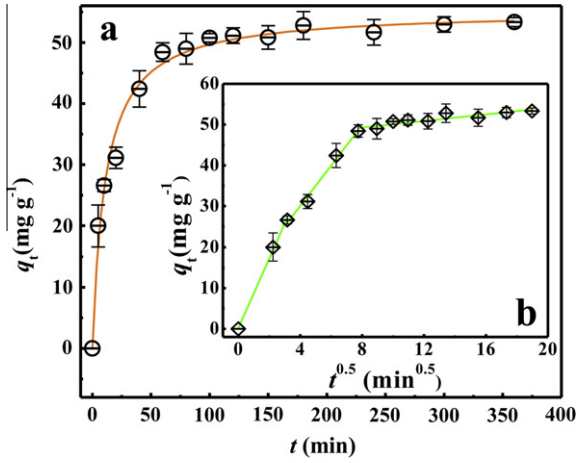

Fig. 4. (a) Pseudo-second-order sorption kinetics, (b) Intraparticle diffusion kinetics. m/V = 0.18 g L^{-1}, pH = 5.0, T = 30 °C, C_0 = 50 mg L^{-1}.

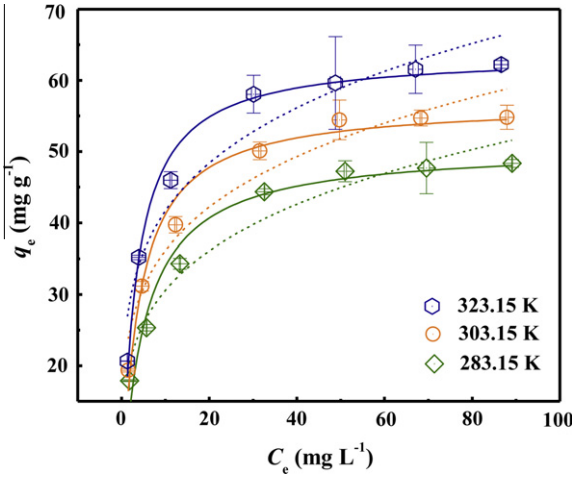

Fig. 5. Langmuir and Freundlich non-linear plots of adsorption isotherms for Cu(II) onto the SMGO at 283.15, 303.15, and 323.15 K. The solid lines are Langmuir model simulation, and the dashed lines are Freundlich model simulation. m/V = 0.18 g L^{-1}, pH = 5.0, t = 6 h.

the rate-controlling step [37,38]. In this case, the plot was multilinear over the whole time range, implying that more than one process affected the adsorption. The initial portion related to the boundary layer diffusion (film diffusion), and the second portion described the gradual adsorption step, where the intraparticle diffusion is the rate-limiting step. The third linear portion indicated the adsorption–desorption equilibrium. Therefore, film diffusion and intraparticle diffusion were simultaneously occurring during the adsorption process, and the intraparticle diffusion was not the only rate controlling step for the whole process. Similar behavior was obtained by Zhang et al. [39] in the adsorption of Rhenium ions onto modified nano-Al_2O_3.

3.4. Adsorption isotherms and thermodynamics

The Freundlich and Langmuir adsorption isotherms obtained using the non-linear method at 283.15, 303.15, and 323.15 K are shown in Fig. 5, and the isotherm constants as well as the coefficients of determination are shown in Table 3. From Fig. 5 and Table 3, we can see that the experimental data are fitted better by the Langmuir model than by the Freundlich model within the studied temperature range, suggesting that Cu^{2+} is adsorbed by specific sites of SMGO and forms monolayer [8]. The value of q_{max} at different temperatures 283.15, 303.15, and 323.15 K were found to be 50.678, 56.857, and 63.670 mg g^{-1}, respectively. Both q_{max} and K_L of the Langmuir model increased with increase in temperature, indicating the bonding between Cu(II) and active sites of the adsorbent weakened at lower temperature and the adsorption process is endothermic [11]. The q_m is 56.857 mg g^{-1} at 303.15 K, which is higher than that of GO (46.6 mg g^{-1} at room temperature and pH = 5) [8], GO aerogels (29.59 mg g^{-1} at 313.15 K and pH = 6.3) [33] and carbon nanotubes (28.49 mg g^{-1} at room temperature and pH = 5) [40]. The huge adsorption capacity might owe to the abundant oxygen-containing functional groups and large surface (92.79 m^2 g^{-1}) of SMGO. On the other hand, the introduction of abundant $-SO_3H$ groups to the sp^2 carbon network was another cause.

Plot of ln$K°$ versus 1/T for Cu(II) adsorption on SMGO is shown in Fig. S1 (Supplementary Data). The thermodynamic parameters calculated at three different temperatures are listed in Table 4. The negative $\Delta G°$ (−20.196 kJ mol^{-1} at 283.15 K, −22.273 kJ mol^{-1} at 303.15 K, and −24.349 kJ mol^{-1} at 323.15 K) indicated that the adsorption was a spontaneous process under the conditions applied, and the value of $\Delta G°$ became more negative with the increase of temperature, indicating that higher temperature facilitated the adsorption process [21]. The obtained positive $\Delta H°$ value (9.205 kJ mol^{-1}) suggests an endothermic adsorption mechanism, which is in good agreement with the results that the adsorption of Cu(II) increases with the increasing temperature (Fig. 5). $\Delta S°$ (103.835 J mol^{-1} K^{-1}) is also positive, which implies that adsorption process is spontaneous with high affinity. It also suggests that there are some structural changes in both the adsorbate and adsorbent [6]. Above all, it can be concluded that the adsorption of Cu(II) on the SMGO is an endothermic and spontaneous process.

Table 3
Langmuir and Freundlich isotherm parameters for Cu(II) adsorption on SMGO (m/V = 0.18 g L^{-1}, pH = 5.0, t = 6 h).

Models	Parameters	Temperature (K)		
		283.15	303.15	323.15
Langmuir				
	q_{max} (mg g^{-1})	50.678	56.857	63.670
	K_L (L mg^{-1})	0.203	0.263	0.311
	R^2	0.950	0.973	0.985
Freundlich				
	n	4.181	4.464	4.649
	K_F (L mg^{-1})	17.627	21.574	25.395
	R^2	0.946	0.940	0.923

Table 4
Thermodynamic parameters of Cu(II) adsorption on SMGO (m/V = 0.18 g L^{-1}, pH = 5.0, t = 6 h).

Thermodynamic parameters	Temperature (K)		
	283.15	303.15	323.15
ln $K°$	8.579	8.837	9.063
$\Delta G°$ (kJ mol^{-1})	−20.196	−22.273	−24.349
$\Delta H°$ (kJ mol^{-1})	9.205		
$\Delta S°$ (J mol^{-1} K^{-1})	103.835		

4. Conclusions

The analysis results of TEM, EDS, Particles size, BET, TG-DTA, FT-IR, and Raman indicated that sulfonated magnetic graphene oxide composite was successfully prepared. It can be easily separated by magnetic separation from the medium after adsorption. The introduction of sulfo groups to the GO surface can increase efficiency of

Cu(II) adsorption. The variables (pH, Cu(II) concentrations, and temperature) were successfully optimized by response surface methodology and the maximum predicted value of adsorption capacity was 62.73 mg g^{-1}. The kinetics and isotherm experiment data can be well described with the pseudo-second order model and the Langmuir isotherm model, respectively. The rate controlling mechanism study revealed that film diffusion and intraparticle diffusion were simultaneously occurring during the adsorption process. The thermodynamic parameters indicated that the adsorption reaction of Cu(II) on the SMGO was an endothermic and spontaneous process. Based on these results, it can be concluded that the SMGO is a very suitable material for metal ions pollution cleanup.

Acknowledgements

The authors would like to thank financial support from the National Natural Science Foundation of China (Grant No. 41271332), the Natural Science Foundation of Hunan province, China (Grant No. 11JJ2031) and the Hunan Provincial Innovation Foundation For Postgraduate (Grant No. CX2012B138).

Appendix A. Supplementary material

Supplementary data associated with this article can be found, in the online version, at http://dx.doi.org/10.1016/j.seppur.2013.02.011.

References

[1] M.J. Allen, V.C. Tung, R.B. Kaner, Honeycomb carbon: a review of graphene, Chem. Rev. 110 (2010) 132–145.
[2] G. Chen, S. Zhai, Y. Zhai, K. Zhang, Q. Yue, L. Wang, J. Zhao, H. Wang, J. Liu, J. Jia, Preparation of sulfonic-functionalized graphene oxide as ion-exchange material and its application into electrochemiluminescence analysis, Biosens. Bioelectron. 26 (2011) 3136–3141.
[3] S. Stankovich, D.A. Dikin, G.H.B. Dommett, K.M. Kohlhaas, E.J. Zimney, E.A. Stach, R.D. Piner, S.T. Nguyen, R.S. Ruoff, Graphene-based composite materials, Nature 442 (2006) 282–286.
[4] H. He, J. Klinowski, M. Forster, A. Lerf, A new structural model for graphite oxide, Chem. Phys. Lett. 287 (1998) 53–56.
[5] A. Lerf, H. He, M. Forster, J. Klinowski, Structure of graphite oxide revisited, J. Phys. Chem. B 102 (1998) 4477–4482.
[6] G. Zhao, J. Li, X. Ren, C. Chen, X. Wang, Few-layered graphene oxide nanosheets as superior sorbents for heavy metal ion pollution management, Environ. Sci. Technol. 45 (2011) 10454–10462.
[7] H.L. Ma, Y. Zhang, Q.H. Hu, D. Yan, Z.Z. Yu, M. Zhai, Chemical reduction and removal of Cr(VI) from acidic aqueous solution by ethylenediamine-reduced graphene oxide, J. Mater. Chem. 22 (2012) 5914–5916.
[8] S.T. Yang, Y. Chang, H. Wang, G. Liu, S. Chen, Y. Wang, Y. Liu, A. Cao, Folding/aggregation of graphene oxide and its application in Cu^{2+} removal, J. Colloid Interface Sci. 351 (2010) 122–127.
[9] C.J. Madadrang, H.Y. Kim, G. Gao, N. Wang, J. Zhu, H. Feng, M. Gorring, M.L. Kasner, S. Hou, Adsorption Behavior of EDTA-graphene oxide for Pb(II) removal, Appl. Mater. Interfaces 4 (2012) 1186–1193.
[10] S. Bai, X. Shen, X. Zhong, Y. Liu, G. Zhu, X. Xu, K. Chen, One-pot solvothermal preparation of magnetic reduced graphene oxide-ferrite hybrids for organic dye removal, Carbon 50 (2012) 2337–2346.
[11] X.J. Hu, J.S. Wang, Y.G. Liu, X. Li, G.M. Zeng, Z.L. Bao, X.X. Zeng, A.W. Chen, F. Long, Adsorption of chromium (VI) by ethylenediamine-modified cross-linked magnetic chitosan resin: isotherms, kinetics and thermodynamics, J. Hazard. Mater. 185 (2011) 306–314.
[12] J.S. Wang, R.T. Peng, J.H. Yang, Y.C. Liu, X.J. Hu, Preparation of ethylenediamine-modified magnetic chitosan complex for adsorption of uranyl ions, Carbohydr. Polym. 84 (2011) 1169–1175.
[13] L. Zhou, Y. Wang, Z. Liu, Q. Huang, Characteristics of equilibrium, kinetics studies for adsorption of Hg(II), Cu(II), and Ni(II) ions by thiourea-modified magnetic chitosan microspheres, J. Hazard. Mater. 161 (2009) 995–1002.
[14] H. He, C. Gao, General approach to individually dispersed, highly soluble, and conductive graphene nanosheets functionalized by nitrene chemistry, Chem. Mater. 22 (2010) 5054–5064.
[15] P. Kulamani, G.M. Krushna, K.D. Suresh, Adsorption of Copper(II) on NH_2-MCM-41 and Its application for epoxidation of styrene, Ind. Eng. Chem. Res. 51 (2012) 2235–2246.
[16] R.K. Layek, S. Samanta, A.K. Nandi, The physical properties of sulfonated graphene/poly (vinylalcohol) composites, Carbon 50 (2012) 815–827.
[17] G.E.P. Box, D.W. Behnken, Simplex-sum designs-A class of 2nd order rotatable designs derivable of those of 1st order, Ann. Math. Stat. 31 (1960) 838–864.
[18] R. Gao, H. Liu, Z. Peng, Z. Wu, Y. Wang, G. Zhao, Adsorption of (−)-epigallocatechin-3-gallate (EGCG) onto oat β-glucan, Food Chem. 132 (2012) 1936–1943.
[19] Z. Chen, W. Ma, M. Han, Biosorption of nickel and copper onto treated alga (Undaria pinnatifida): application of isotherm and kinetic models, J. Hazard. Mater. 155 (2008) 327–333.
[20] Z. Aksu, Determination of the equilibrium, kinetic and thermodynamic parameters of the batch biosorption of nickel (II) ions onto *Chlorella vulgaris*, Process Biochem. 38 (2002) 89–99.
[21] J. Xu, L. Wang, Y. Zhu, Decontamination of bisphenol a from aqueous solution by graphene adsorption, Langmiur 28 (2012) 8418–8425.
[22] G.X. Zhao, J.X. Li, X.K. Wang, Kinetic and thermodynamic study of 1-naphthol adsorption from aqueous solution to sulfonated graphene nanosheets, Chem. Eng. J. 173 (2011) 185–190.
[23] Y. Yang, J. Wang, J. Zhang, J. Liu, X. Yang, H. Zhao, Exfoliated graphite oxide decorated by PDMAEMA chains and polymer particles, Langmuir 25 (2009) 11808–11814.
[24] L.Z. Bai, D.L. Zhao, Y. Xu, J.M. Zhang, Y.L. Gao, L.Y. Zhao, J.T. Tang, Inductive heating property of graphene oxide-Fe_3O_4 nanoparticles hybrid in an AC magnetic field for localized hyperthermia, Mater. Lett. 68 (2012) 399–401.
[25] C. Hou, Q. Zhang, M. Zhu, Y. Li, H. Wang, One-step synthesis of magnetically-functionalized reduced graphite sheets and their use in hydrogels, Carbon 49 (2011) 47–53.
[26] C. Nethravathi, M. Rajamathi, Chemically modified grapheme sheets produced by the solvothermal reduction of colloidal dispersions of graphite oxide, Carbon 46 (2008) 1994–1998.
[27] A.C. Ferrari, J.C. Meyer, V. Scardaci, C. Casiraghi, M. Lazzeri, F. Mauri, S. Piscanec, D. Jiang, K.S. Novoselov, S. Roth, A.K. Geim, Raman spectrum of graphene and graphene layers, Phys. Rev. Lett. 97 (2006) 187401.
[28] J. Ji, G. Zhang, H. Chen, S. Wang, G. Zhang, F. Zhang, X. Fan, Sulfonated graphene as water-tolerant solid acid catalyst, Chem. Sci. 2 (2011) 484–487.
[29] J. Goel, K. Kadirvelu, C. Rajagopal, V.K. Garg, Cadmium(II) uptake from aqueous solution by adsorption onto carbon aerogel using a response surface methodological approach, Ind. Eng. Chem. Res. 45 (2006) 6531–6537.
[30] R.O. Kuehl, Design of experiments: statistical principles of research design and analysis, second ed., Duxbury press, California, 2000.
[31] Z.H. Huang, X. Zheng, W. Lv, M. Wang, Q.H. Yang, F. Kang, Adsorption of lead(II) ions from aqueous solution on low-temperature exfoliated graphene nanosheets, Langmuir 27 (2011) 7558–7562.
[32] M. Liu, C. Chen, J. Hu, X. Wu, X. Wang, Synthesis of magnetite/graphene oxide composite and application for cobalt(II) removal, J. Phys. Chem. C 115 (2011) 25234–25240.
[33] X. Mi, G. Huang, W. Xie, W. Wang, Y. Liu, J. Gao, Preparation of graphene oxide aerogel and its adsorption for Cu^{2+} ions, Carbon 50 (2012) 4856–4864.
[34] J. Li, S. Zhang, C. Chen, G. Zhao, X. Yang, J. Li, X. Wang, Removal of Cu(II) and fulvic acid by graphene oxide nanosheets decorated with Fe_3O_4 nanoparticles, Appl. Mater. Interfaces 4 (2012) 4991–5000.
[35] Z. Reddad, C. Gerente, Y. Andres, P.L. Cloirec, Adsorption of several metal ions onto a low-cost biosorbent: kinetic and equilibrium studies, Environ. Sci. Technol. 36 (2002) 2067–2073.
[36] Y. Prasanna Kumar, P. King, V.S.R.K. Prasad, Equilibrium and kinetic studies for the biosorption system of copper(II) ion from aqueous solution using *Tectona grandis* L. f. leaves powder, J. Hazard. Mater. 137 (2006) 1211–1217.
[37] S. Svilović, D. Rušić, A. Bašić, Investigations of different kinetic models of copper ions sorption on zeolite 13X, Desalination 259 (2010) 71–75.
[38] X. Wang, L. Shu, Y. Wang, B. Xu, Y. Bai, S. Tao, B. Xing, Sorption of peat humic acids to multi-walled carbon nanotubes, Environ. Sci. Technol. 45 (2011) 9276–9283.
[39] L. Zhang, X.Q. Jiang, T.C. Xu, L.J. Yang, Y.Y. Zhang, H.J. Jin, Sorption characteristics and separation of rhenium ions from aqueous solutions using modified nano-Al_2O_3, Ind. Eng. Chem. Res. 51 (2012) 5577–5584.
[40] Y.H. Li, J. Ding, Z. Luan, Z. Di, Y. Zhu, C. Xu, D. Wu, B. Wei, Competitive adsorption of Pb^{2+}, Cu^{2+} and Cd^{2+} ions from aqueous solutions by multiwalled carbon nanotubes, Carbon 41 (2003) 2787–2792.